Indian Journal of Engineering & Materials Sciences
Vol. 30, December 2023, pp. 805-815
DOI: 10.56042/ijems.v30i6.2182

Machine Learning Approach to the Prediction of Surface Roughness of Turned Glass/Basalt Epoxy Composites

Amith Gadagi* & Chandrashekar Adake

KLE Technological University's Dr.MSSCET, Depatment of Mechanical Engineering, Belagavi, 590008, India.

Received: 31 May 2023; Accepted: 21 November 2023

In this work, the Machine Learning techniques namely Support Vector Regression, Random forest methodand Extreme Gradient Boosting (XGBOOST) are utilized for the prediction of Surface Roughness in the turning process of Glass/Basalt epoxy hybrid composites. The experiments were conducted in accordance with the Taguchi's L27 orthogonal array. The experimental results indicates that, the surface roughness of the turned Glass/Basalt epoxy composites decreases with the increase in Spindle speed, decrease in Feed rate and Depth of cut. It was also observed that feed rate has a greatest impact and Depth of cut has a least effect over the surface roughness while the spindle speed moderately influenced the surface roughness. From the results of Machine Learning models, it is evident that the Random forest model appears to be superior with a Mean Absolute error and Maximum error of 4.96% and 7.73% respectively for testing data set.

Keywords: Composites, Production, Turning, Surface Roughness, Machine Learning

1 Introduction

The primary emphasis in the aviation, automotive and marine industries is to develop and apply composite materials that has high strength and less weight. Glass-Basalt/epoxy hybrid composite specimens were prepared by Fiore et al. for Marine applications and also evaluated the effect of layers on the mechanical performance. A vacuum bagging Technique was employed to manufacture the specimens and Tensile, Three point bending tests were conducted to evaluate the Mechanical properties. Further, their work also included the development of the experimentally validated numerical model for the estimation of mechanical properties[1] . Ramraji et al., made an attempt to cut Basalt Finer/Fly ash polymer composites by using Abrasive Water jet machining. It was observed that, the damage due to fiber pull out was minimized with the increase in the intensity of jet pressure[2]. Rajesh et al., conducted experimental studies on abrasive jet water machining of Ti metal-interleaved basalt-flax fiber laminates. RSM based empirical modeling of surface roughness, kerf ratio was done and prediction done through both the empirical models were found to be in good agreement with the experimental values[3]. Amuthakkannan et al., utilized the technique of abrasive water jet machining to cut the polymer based Basalt Fiber Composites. Experiments were conducted to find the kerf angle, bottom kerf, top kerf by considering the machining parameters namely water pressure, speed of nozzle and stand off distance. Grey relational analysis was used to arrive at the optimal machining parameters to obtain the better performance indicators[4]. Jain et al. carried out the laser cutting of basalt and glass based flat composite laminates by considering process variables namely Pulse frequency, Lamp current, Pulse width, cutting speed and Air gas pressure. RSM based cubic and quadratic empirical models were developed for the performance indicators Top kerf deviation and Bottom kerf deviation. The developed models predicted the performance indicators very well with a minimum deviation as compared to the corresponding experimental values[5] . Tan et al., conducted the drilling studies to investigate the effect of process parameters on surface roughness and delamination of hybrid carbon-glass composites[6] . Navarro et al., conducted the study on delamination of Basalt Fiber Reinforced Plastics in a Edge trimming process. Delamination was found to occur in all the specimens with a fiber volume of 60% and also the higher tool wear did not allow to machine the material because of severe delamination[7]. Patel et al., conducted the drilling studies on hybrid basalt/glass polyester composite samples by considering Feed, speed, Tool geometry and stacking sequence as the independent process variables. The response variables

*Corresponding author (E-mail: amithgadagi@gmail.com)

considered were delamination at the bottom, delamination at the top and the thrust force. A Design of experiments based approach was employed for experimentation and a Grey Relational Analysis technique was utilized to arrive at the optimal machining condition[8] . Dutt et al., investigated the effect of laser cutting of Kevlar-Basalt fiber composite on the kerf taper, kerf deviation, kerf width by considering pulse frequency, pulse width, lamp current, cutting speed and pressure of the compressed air as the process parameters. It was concluded that, lower levels of process parameters would result in a narrow kerf width along with the red taper and deviation[9]. Sathish kumar et al., utilized the technique of abrasive water jet machining in drilling of Basalt–Kevlar–Glass fiber reinforced polymer cross ply laminate. The process parameters considered were stand-off distance, abrasive mass flow rate, traverse speed and response parameters namely surface finish, kerf taper, material removal rate were optimized using response surface methodology. The optimized results were found to be in close match with the experimental results[10] . Mustafa et al. investigated the influence of parameters like abrasive mass flow rate, standoff distance, traverse speed, material thickness and pressure on surface roughness and kerf width in abrasive water jet cutting of glass-vinyl ester composite. ANOVA results suggested that, standoff distance was the most significant process parameter[11]. Joshi et al. conducted the drilling study of Glass fiber reinforced plastic to examine the effect of drilling mode, feed and cutting speed on hole oversize and delamination factor. It was concluded that, the feed was significant for all the modes of drilling[12] .Navarro et al., conducted the tool wear studies of uncoated carbide inserts in the edge trimming of a basalt fiber reinforced plastics by considering the cutting conditions namely depth of cut, feed and speed. Also material characteristics namely Fiber orientation and volume fraction were considered in the conduction of tool wear studies. Their work was mainly focused on Material removal rate, flank wear and the development of corresponding empirical model[13].

Nima et al, predicted the fugitive landfill gas hotspots with the help of Random forest method . Their study also involved the mapping of fugitive gas emission hot spots with a higher spatial resolution[14] . Yuan et al, successfully employed Random forest method for the estimation of carbon emissions at construction stage and was helpful in finding the problems at design stage[15]. Khan et al., utilized the concept of random forest to predict the salinity of surface water bodies by considering the independent variables as total disolved solids and electrical conductivity[16]. Djandja et al., developed the model to predict the phosphorus content in hydochar obtained from a hydrothermal carbonization of sewage sludge with the help of Random forest algorithm with a better accuracy. The input parameters considered were reaction time, temperature initial pH and ash content[17] . Tojal et al achieved an R^2 more than 0.7 in predicting the above ground biomass with the use of random forest technique The model predicted the biomass data 16 to 18% higher than that of data as per Basque government[18] . In the field of machine learning technique several researchers have utilized Support vector Regression[19-23] and Extreme gradient boosting method[24-28]for the computational purposes.

The literature presented in this paper suggests that the turning process of Glass/Basalt epoxy composites has never been carried out, so their performance characteristics were never been investigated. Considering this as a research gap, the turning process performance characteristics of Glass/Basalt epoxy composites are investigated in this work. Also the Multiple regression model, machine learning models such as Support vector Regression,Random forest method and Extreme gradient boosting method are developed and their computational performances are compared in this work.

2 Materials and Methods

2.1 Experimental method

In this work, the Basalt/glass epoxy composite bars of outer diameter 55 mm, which are required for turning operation, are fabricated using Basalt and glass fiber mesh. Lapox L-12 epoxy resin is used along with K-6 hardener and silicon carbide fillers (5% of resin by weight). Basalt fiber mesh and Glass fiber mesh are cut appropriately,appropriate amount of resin is applied on glass fiber mesh and then basalt fiber mesh is added on glass fibermesh. Further the resin is applied on basalt fiber mesh,alternate stacking of glass and basalt fiber meshes with the application of resin is done till the composite pipe of desired outer diameter is obtained. Fig. 1(a) shows the Basalt fiber and Glass fiber mesh and Fig. 1(b) shows silicon carbide filler powder. The resin which is mixed with the silicon carbide filler powder is shown in Fig. 1 (c). The resin applied fiber meshes as per 1(d) are wrapped on the mandrel of diameter 45 mm as shown in Fig.1 (e). The wound fabric was cured in the hot air

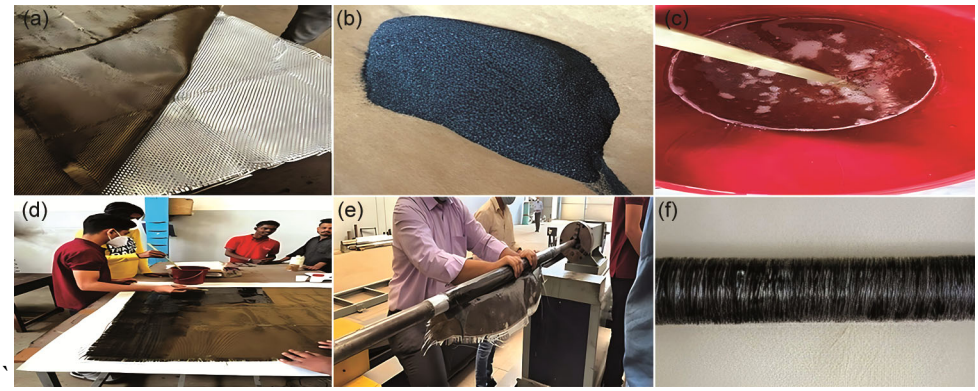

Fig. 1— Fabrication of Basalt/glass epoxy composite bars: (a) Basalt and Glass Fibre mesh, (b) Sic filler, (c) Epoxy Resin, (d) application of Resin over the mesh, (e) Rolling of material over the mandrel, & (f) Final composite pipe.

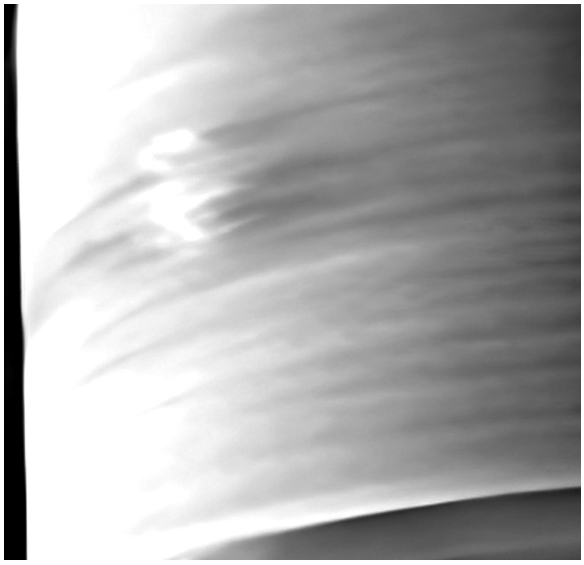

Fig. 2 — Machined Basalt/glass epoxy composite specimen.

Fig. 3 — BFW CNC Orbitur Machine.

Fig. 4 — TNMG 160408 NN LT 10carbide cutting insert.

circulating ovenand after curing, the mandrel is extracted by means of hydraulic extractor. The final composite pipe manufactured is as shown in Fig.1 (f).

The machined Basalt/glass epoxy composite specimen, which is as shown in Fig. 2, is obtained by turning on a BFW ORBITUR CNC Turning center using carbide cutting insert of grade TNMG 160408 NN LT 10. The Fig. 3 shows the CNC Turning center and the insert used is as shown in Fig. 4. The surface roughness of the turned Basalt/glass epoxy composite specimens are measured using Surfcom Flex 50A surface tester machine.

The turning experiments are conducted according to Taguchi's L27 Full Factorial orthogonal array by considering Depth of cut, Spindle speed and Feed rate as the process parameters. The details of the levels chosen for the generation of Taguchi's L27 array are mentioned in Table 1 and the complete information of the Design of experiments (DOE) is given in Table 2. The details of the conformal experiments which are used for the validation of Machine learning models are given in Table 3.

Table 1 —Details of Levels used in DOE

Levels	Spindle Speed (RPM)	Feed rate (mm/rev)	Depth of cut (mm)
1	400	0.05	0.3
2	800	0. 1	0.6
3	1200	0. 15	1.0

Table 2 — Details of Taguchi's L27 array

Experiment No.	Spindle Speed (RPM)	Feed rate (mm/rev)	Depth of cut (mm)	Experimental Ra (μm)
1	400	0.05	0.3	2.7410
2	400	0.05	0.6	2.6623
3	400	0.05	1	2.8530
4	400	0.1	0.3	3.1180
5	400	0.1	0.6	3.2040
6	400	0.1	1	3.2146
7	400	0.15	0.3	3.4120
8	400	0.15	0.6	3.2943
9	400	0.15	1	3.2403
10	800	0.05	0.3	2.5293
11	800	0.05	0.6	2.5536
12	800	0.05	1	2.6350
13	800	0.1	0.3	2.7960
14	800	0.1	0.6	2.8396
15	800	0.1	1	3.0306
16	800	0.15	0.3	3.2800
17	800	0.15	0.6	3.3096
18	800	0.15	1	3.3413
19	1200	0.05	0.3	2.3380
20	1200	0.05	0.6	2.3760
21	1200	0.05	1	2.4273
22	1200	0.1	0.3	2.7260
23	1200	0.1	0.6	2.7490
24	1200	0.1	1	2.8206
25	1200	0.15	0.3	3.5510
26	1200	0.15	0.6	3.6610
27	1200	0.15	1	3.5800

Table 3 — Details of conformal experiments (Testing data set)

Experiment No.	Spindle Speed (RPM)	Feed rate (mm/rev)	Depth of cut (mm)	Experimental Ra (μm)
1	400	0.1	0.4	3.1796
2	750	0.085	0.5	3.0673
3	1075	0.05	0.65	2.5850
4	800	0.075	0.4	2.9893
5	1050	0.08	0.35	2.5556
6	975	0.05	0.75	2.6316
7	900	0.07	0.9	2.6873

2.2 Machine learning Techniques

Machine learning, a subset of artificial intelligence, is that area of computational study which enables the computer to make predictions in real time scenarios. The machine learning may be categorized into supervised, unsupervised, semi-supervised and reinforcement learning methods. In this work, the supervised learning technique is used which uses both the input and output data from the experimental history. The machine learning techniques used in study are Support Vector Regression, R and om Forest and Extreme gradient boosting method. Implementation of both the machine learning algorithms are done in Jupyter Note Book and the code is written using Python programming language.

2.3 Support Vector Regression

Support Vector Regression (SVR) is basically a classification of Support vector Machine and a supervised machine learning model. The use of a Kernel term in this model makes it more in dealing with the nonlinearity aspects associated with the process. SVR evaluates a real valued function by getting trained with a symmetrical loss function by penalizing high and low error estimates with the equal weights. SVR by using an Vapnik's technique forms a flexible tube with minimum diameter symmetrically following an estimated function such that error estimates below the threshold valued are discarded. The data points falling outside the flexible tube are penalized whilst those which are inside does not receive any penalization. In Support Vector Regression ε-tube, an ε-insensitive domain surrounding the estimated function, optimizes its shape by weighing the error in prediction and complexity of the model equally. By considering the loss function and geometrical parameters of tube, a multi objective function for the optimization is formulated. It is minimized such that a flattest possible tube is obtained, which is comprising of maximum instances of training. SVR determines an optimal hyper plane from which all the data instances are at a minimum distances[29] .

The dependent and independent parameters in SVR are related by Eq. 1

$$D = f(I) = W\, x\, \emptyset(I) + B \qquad \ldots (1)$$

D = dependent factor, I = independent factor, W = Weight matrix, B = Constant, $\emptyset(I)$ = high-dimensional space with a highly nonlinear mapping.

The minimization of a regularized function in SVR is done using as per Eq 2.,

Minimize:

$$M(f) = \gamma \frac{1}{Q}\sum_{R=1}^{R=J}(\delta_R + {\delta_R}^*) + \frac{1}{2}W^2 \begin{cases} D_j - wx\emptyset(I_j) - B \le (\delta + \delta_j) \\ wx\emptyset(I_j) + B - D_i \le \delta + \delta_R^* \\ \delta_R, \delta_R^* \ge 0 \end{cases} \quad \ldots (2)$$

By using the kernel function $K(I, I_R)$and Lagrangian multipliers (α_R, α_R^*) , solution for Eq 3. can be expressed as,

Table 4 —Details of SVR model parameters

Parameter	Details
Penalty parameter (C)	10000
Kernel	Radial basis function
Gamma	0.5
Epsilon	0.07

Maximize: $-\frac{1}{2}\sum_{R=1}^{R=m} 1 \sum_{R=1}^{R=m}(\alpha_R - \alpha_R^*)(\alpha_P - \alpha_P^*)K(I_R, I_P) - \varepsilon \sum_{R=1}^{R=m}(\alpha_R - \alpha_R^*) + \sum_{R=1}^{R=m} D_R(\alpha_R - \alpha_R^*)$ … (3)

Constraints: $\begin{cases} \sum_{R=1}^{R=m}(\alpha_R - \alpha_R^*) = 0 \\ \alpha_R, \alpha_R^* \varepsilon (0, \gamma) \end{cases}$

The solution for the above equation can be written as,

$$D = f(I) = (\alpha_R - \alpha_R^*)xK(I, I_R) + B \quad \ldots (4)$$

The details of the SVR algorithm parameters are given in Table 4.

The comparison of SVR results with the experimental results of surface roughness for the training and testing data sets are done in Fig. 5 and Fig. 6 respectively.

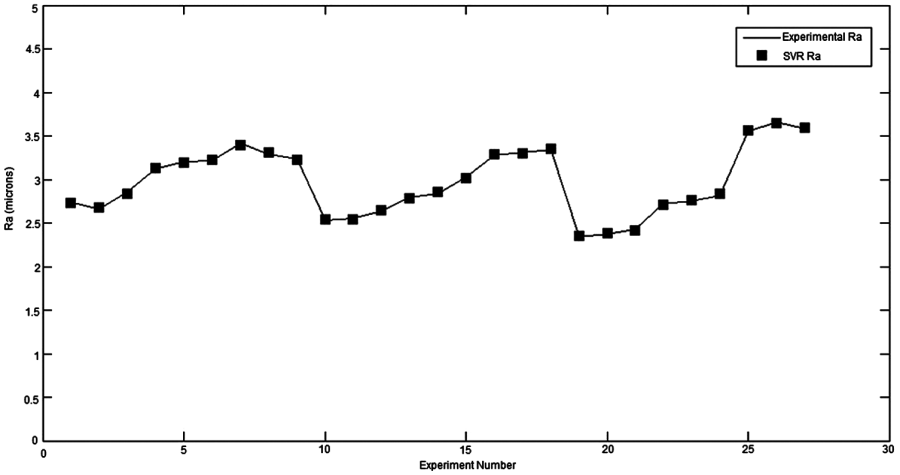

Fig. 5 — SVR and Experimental comparison plot of Surface Roughness of turned Basalt/glass epoxy composites for training data set.

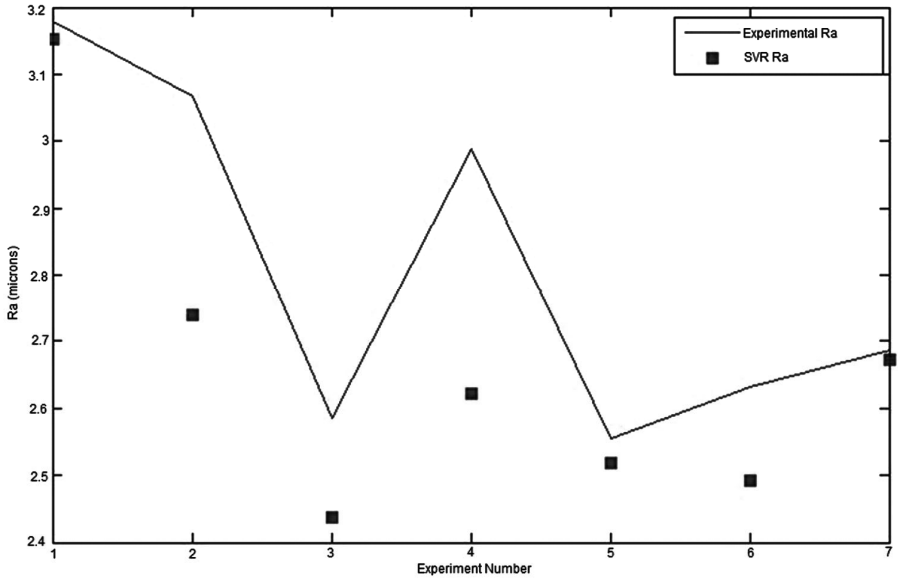

Fig. 6 — SVR and Experimental comparison plot of Surface Roughness of turned Basalt/glass epoxy composites for testing data set.

For SVR model, the maximum error of surface roughness is found to be 0.01 μm and 0.367 μm for training and testing data set respectively. The average surface roughness error for training and testing data set is 0.01 μm and 0.151 μm respectively.

2.4 Random Forest

Random forest falls under a category of ensemble technique, which basically performs classification and regression tasks by using aggregation and bootstrap techniques. Bootstrapping involves random row and feature sampling while the aggregation involves combining the predictions done by various decision trees. The combination of aggregation, bootstrapping is called as bagging technique and also the multiple decision trees are used in Random forest algorithm. Each decision tree comprises of the components such as root node, decision nodes and leaf nodes. In the execution of Random forest algorithm the root nodes are split into decision nodes and the nodes which cannot be split further are termed as leaf nodes. The criteria involved in splitting of the nodes are the values of Gini index and entropy. Gini index and entropy are calculated as per Eq. 5 and Eq. 6 respectively.

$$\text{Gini index} = 1 - \sum_{q=1}^{q=n} (p_q)^2 \quad \ldots (5)$$

where p_q = probability of each class and n = node

$$\text{Entropy} = -\sum_{q=1}^{q=n} p_q log_2 (p_q) \quad \ldots (6)$$

The average prediction of all the multiple decision trees determines the final value of the output in case of regression task while the concept of majority voting is used in case of classification task. The main advantages associated with the Random forest algorithm are its computational speed, reduced overfitting issues and its higher accuracy even though a large amount of training data is missing. Random forest algorithm always tries to achieve low bias and low variance thus eliminating the overfitting issues.

The steps involved in implementing the Random forest algorithm are as follows,

i. Selection of 'n' data instances from the training data set.
ii. Building the 'd' number of decision trees.
iii. Each decision tree draws the 'n' data instances randomly. This process is called bootstrapping.
iv. Growth of the tree takes place by splitting of the nodes through splitting criteria.
v. The prediction done by each decision tree is averaged to calculate the final output and this process is called as aggregation. The final output is of the form as expressed in Eq. 7

$$\bar{\theta} = \frac{1}{d} \sum_{q=1}^{q=d} \theta_q(n) \quad \ldots (7)$$

where θ_q = prediction of a single tree and $\bar{\theta}$ = average prediction of all the decision trees.

The details of the Random forest algorithm parameters are given in Table 5.

The comparison of Random forest results with the experimental results of surface roughness for the training and testing data sets are done in Fig. 7 (a) and 7(b) respectively.

From Fig. 7 (a) and (b) for Random forest model, the maximum error of surface roughness is found to be 0.06 μm and 0.214μm for training and testing data set respectively. The average surface roughness error

Table 5 — Details of Random forest model parameters

Parameter	Details
n_estimators	1000
bootstrap	True
criterion	mse
random_state	None
verbose	0

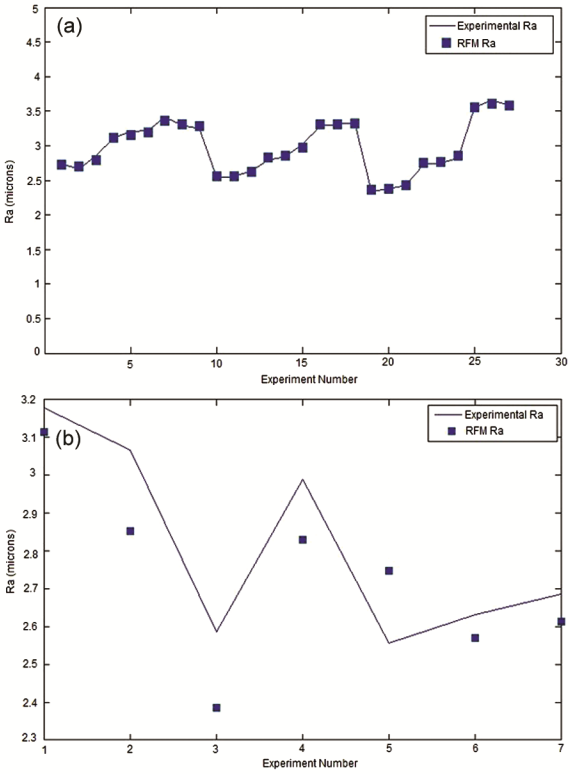

Fig. 7 — Random forestand experimental comparison plot of Surface Roughness of turned Basalt/glass epoxy composites: (a) training data set, & (b) testing data set.

for training and testing data set is 0.02 μm and 0.138μm respectively.

2.5 XGBOOST

Extreme Gradient boosting popularly known as XGBOOST is a gradient based decision tree machine learning algorithm which basically aims at making weak learning algorithm a strong learning algorithm. It is basically an optimal incremental technique which is confined to a functional space. In this method a new learner evolves from a base learner using the residuals of the later. The prediction made by the algorithm in every step is equal to the sum of prediction of a second learner and prediction of a previous step. Like this the algorithm iterates till the training error turns out to be very minimal. The regular term present in the XGBOOST makes it more efficient compared to the conventional Gradient boosting algorithm in overcoming the problems of overfitting and also increases the generalization ability. The learning strategy of the XGBOOST method is to maximize the gain when the splitting of a leaf node takes place.

Steps involved in execution of XGBOOST algorithm are as follows,

i. Calculation of the residuals based on the initial guess.
ii. Building of an XGBOOST tree.
iii. Pruning of trees.
iv. Calculation of the prediction of each leaf.
v. Calculation of new predictions.
vi. Calculation of new residuals based on the newer values of prediction.
vii. Iterate over steps 2 to 6, till the loss is found to be minimized.

The loss function that gets minimized in each iteration is given by Eq. 8,

$$\text{Loss function} = \sum_{j=1}^{j=n} l\left(y_j, \varphi_t(x_j)\right) + \sum_{i=1}^{i=I} L(h_i) \quad \ldots (8)$$

where y_j = output,x_j = input, L = regularization term, h_i = hessian at ith iteration.

The details of the XGBOOST algorithm parameters are given in Table 6.

The comparison of XGBOOST results with the experimental results of surface roughness for the training and testing data sets are done in Fig. 8(a) and Fig. 8(b) respectively.

From Fig. 8 (a) and 8 (b) for XGBOOST model, the maximum error of surface roughness is found to be 0. 002 μm and 0.224 μm for training and testing data set respectively. The average surface roughness error for training and testing data set is 0.001 μm and 0. 14 μm respectively.

3 Results and Discussion

In this section of the paper, the effect of all the process variables such as Depth of cut, feed rate and Spindle Speed on the surface roughness of the turned Basalt/Glass epoxy composite specimens are investigated through Analysis of Variance (ANOVA). The details of ANOVA are given in Table 7,

Table 6 — Details of XGBOOST model parameters

Parameter	Details
base_score	0.5
booster	gbtree
colsample_bylevel	1
colsample_bytree	1
gamma	0
learning_rate	0.3
max_depth	6
n_estimators	100
objective	reg:linear

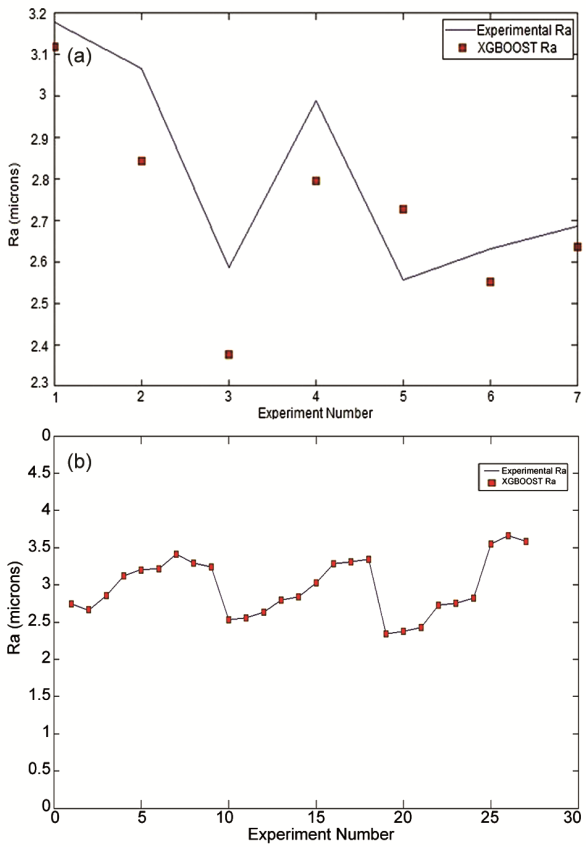

Fig. 8 —XGBOOST and Experimental comparison plot of Surface Roughness of turned Basalt/glass epoxy composites: (a) training data set & (b) testing data set.

Table 7 — ANOVA details

Source	DF	Adj SS	Adj MS	F-Value	P-Value
Regression	3	3.32151	1.10717	42.89	0.000
Spindle Speed	1	0.12677	0.12677	4.91	0.037
Feed Rate	1	3.17016	3.17016	122.80	0.000
Depth of cut	1	0.02458	0.02458	0.95	0.339
Error	23	0.59376	0.02582		
Total	26	3.91527			

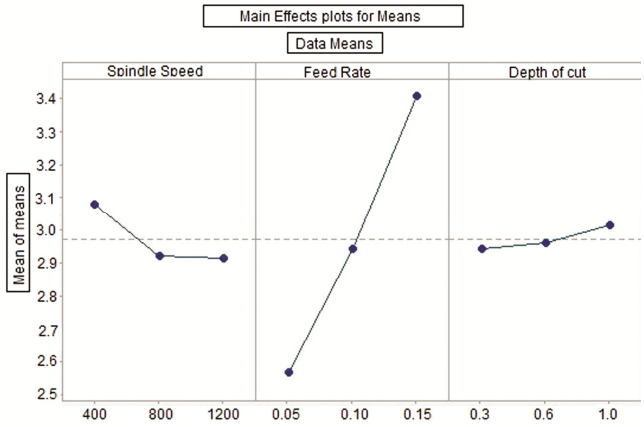

Fig. 9 — Effect of Spindle speed, Feed rate and Depth of cut on Surface Roughness of turned Basalt/glass epoxy composites.

according to which the feed rate and spindle speed has a significant effect on the surface roughness since the corresponding P-Values are less than 0.05. The depth of cut has an insignificant effect on the surface roughness because of its P-Value greater than 0.05.

According to the main effects plot as shown in Fig. 9 as the spindle speed increases the magnitude of the surface roughness decreases and the increase of Feed rate, Depth of cut leads to the increase in surface roughness.

Figure 10 shows the interaction plot of Feed rate and Spindle speed versus Surface roughness in 2D as well as 3D, according to which at a constant feed rate as the spindle speed increases the surface roughness decreases and also at a constant spindle speed if the feed rate increases the surface roughness increases.

The interaction plot of Depth of cut and Spindle speed versus Surface roughness in 2D and 3Dis given in Fig. 11. It can be seen from the Fig. that, if the Spindle speed is held constant and as Depth of cut increases the surface roughness almost remains same and also at a constant Depth of cut if the Spindle speed increases the surface roughness decreases marginally.

Figure 12 gives the interaction plot of Depth of cut and Feed rate versus Surface roughness in 2D as well as 3Dfrom which we can depict that, at a constant

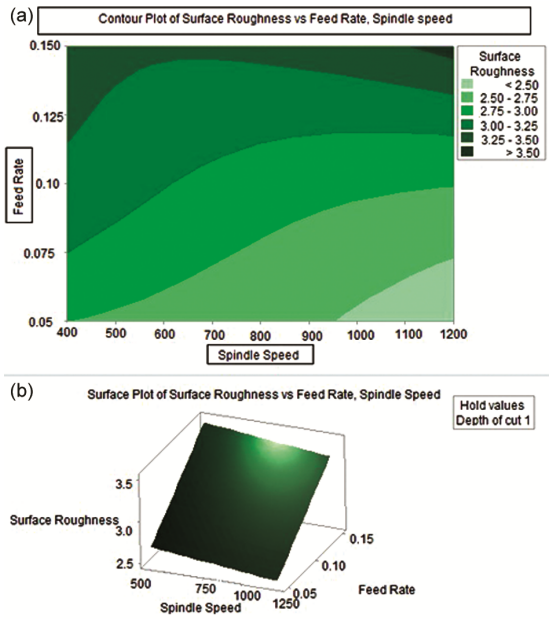

Fig. 10 — Plot of Interaction effect of Spindle speed and Feed rate on Surface Roughness of turned Basalt/glass epoxy composites: a) 2D contour, & b) 3D plot

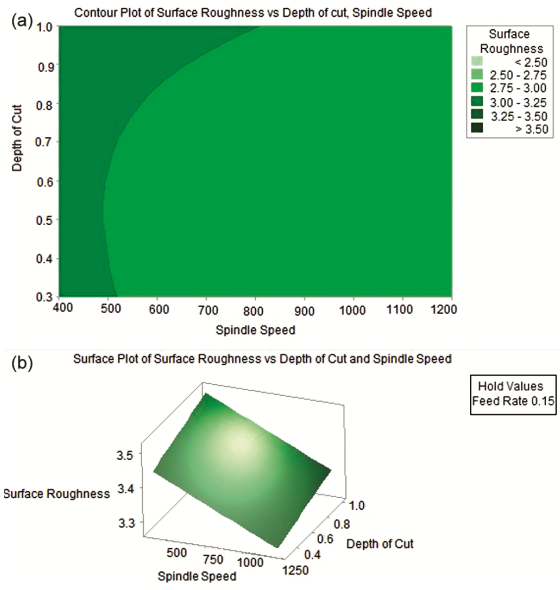

Fig. 11 — Plot of Interaction effect of Spindle speed and Depth of cut on Surface Roughness of turned Basalt/glass epoxy composites: a) 2D contour, & b) 3D plot.

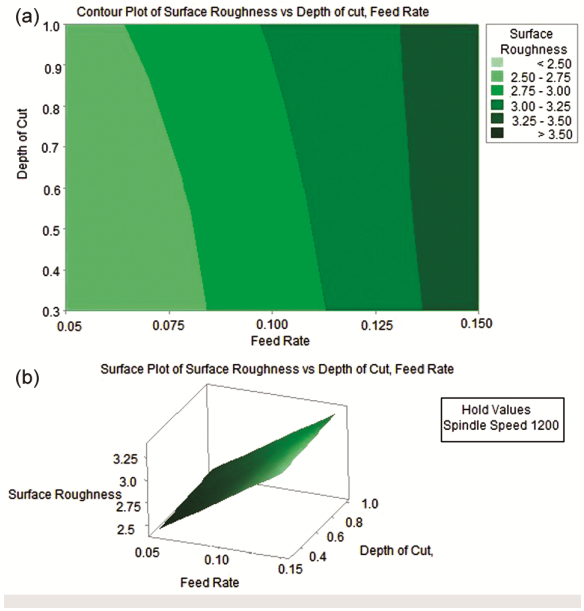

Fig. 12 — Plot of Interaction effect of Feed rate and Depth of cut on Surface Roughness of turned Basalt/glass epoxy composites: a) 2D contour, & b) 3D plot.

feed rate as the depth of cut increases the surface roughness increases marginally and also at a constant Depth of cut if the feed rate increases the surface roughness increases.

The mean absolute percentage error of Training and Testing data sets for all the computational models are given in Fig. 13 (a) and 13 (b) respectively. Figure 14 (a & b) represents the Maximum Percentage error of Training and Testing data sets respectively for all the models.

Percentage error is calculated by Eq. 10,

$$\text{Percentage error} = \frac{(PredictedValue - ExperimentalValue)\times 100}{ExperimentalValue} \quad \ldots (10)$$

From Fig. 13 (a) it can be depicted that, the Mean absolute percentage error in case of training data set for SVR, RFM and XGBOOST models are 0.45%, 0.87% and 0.03% respectively. For the testing data set Mean absolute percentage error corresponding to SVR, RFM and XGBOOST models are found to be 5.26 %, 4.96%and 5.06% from Fig. 13 (b). It can be observed from Fig. 14 (a) that, Maximum Percentage error for SVR, RFM and XGBOOST models are 0.56%, 2.04% and 0.09% for training data set. From Fig. 14 (b). , the Maximum Percentage error are 12.29%, 7,73% and 8.06% for SVR, RFM and XGBOOST models in case of testing data set.

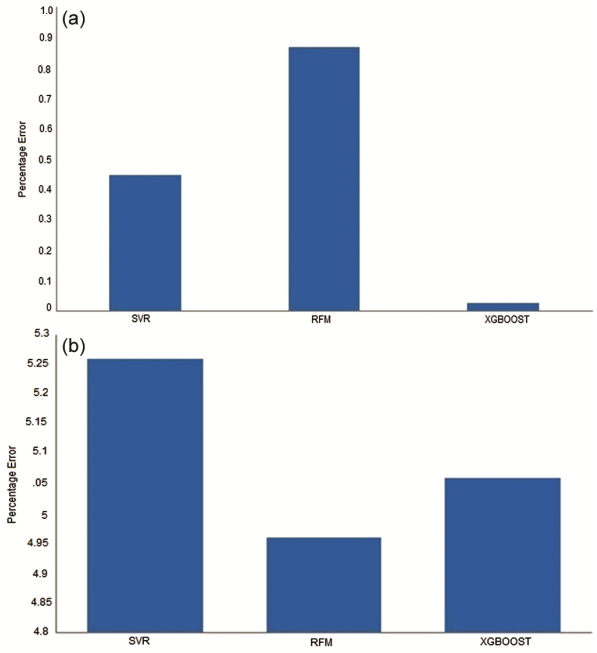

Fig. 13 — Comparison of Mean absolute error (%) of all the computational models: (a) Training data set, & (b) Testing data set.

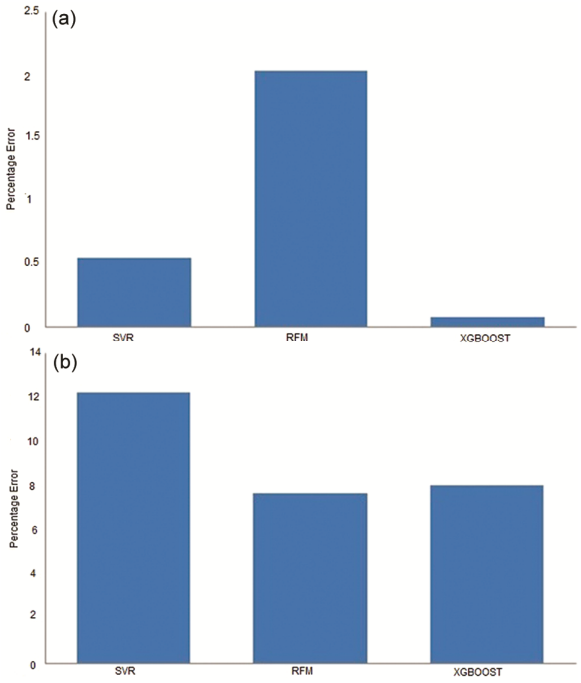

Fig. 14 — Comparison of Maximum Percentage error of all the computational models: (a) Training data set, & (b) Testing data set.

Random forest performed better because of its bootstrapping technique where the final predicted output is based on the combined effect of many regression models. The higher computational

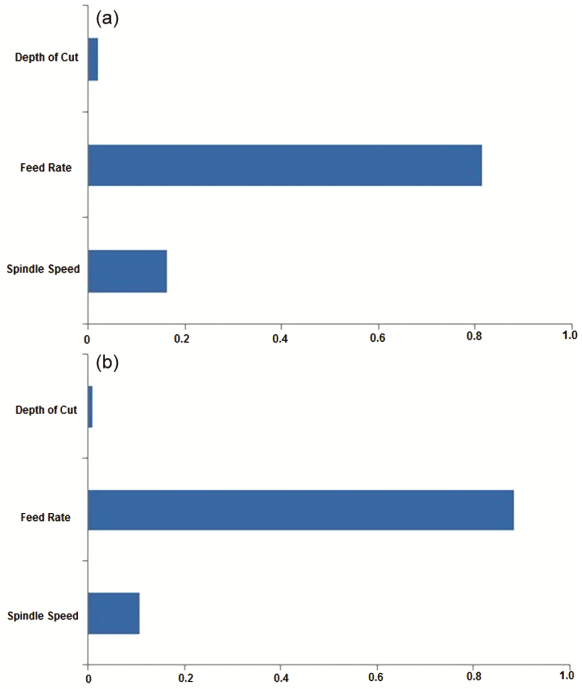

Fig. 15 — Machine learning Feature importance plot: (a) RFM, & (b) XGBOOST.

efficiency of XGBOOST can be attributed to the associated regularization term and sequential learning where the strong learners will be developed from weak learners.

Figure 15, shows aFeature importance plot for RFM and XGBOOST Machine learning models, according to which the Feed rate has a greater influence followed by Spindle speed and Depth of cut.

4 Conclusion

In this work, the effect of turning process parameters namely Spindle Speed, depth of cut and feed rate on surface roughness of the Glass/Basalt epoxy composites is investigated through ANOVA. Further in this study, the computational models such as Support vector Regression, Random forest and XGBOOST are developed for the prediction of surface roughness. Based on these studies, following conclusions are derived,

- ANOVA results suggests that, both the feed rate and spindle speed has a significant effect on surface roughness while the depth of cut is found to be insignificant.
- Through the machine learning feature importance technique, it is observed that feed rate has a highest effect on the surface roughness of the turned Basalt/Glass epoxy composites followed by Spindle speed and Depth of cut.
- The experimental results indicate that, the surface roughness of the turned Basalt/Glass epoxy composites decreases with the decrease of Feed rate, increase in spindle speed and decrease of depth of cut.
- Both the Machine learning computational models namely Random forest and XGBOOST predicted the surface roughness accurately in comparison with SVR.
- The accuracy of Random forest Algorithm predicted results are found to be accurate than the computational results of XGBOOST.

References

1 Fiorea V, Bellab G D &Valenza A, *Mater Des,*32(2011) 2091.
2 Ramraji K, Rajkumar K, Dhananchezian M & Sabarinathan P Composite, *Mater Today Proc*.2(2020) 1351.
3 RajeshM, RajkumarK&AnnamalaiVE*Mater. Manuf. Process,* 36 (2021) 329.
4 Amuthakkannan P, Manikandan V,Uthayakumar M, Arun Prasath K & Sureshkumar S, *Mater Phys Mech,*47 (2021) 830.
5 AkshayJ & Bhagat S, Parametric *Lasers Manuf Mater,*7 (2020) 111.
6 TanCL, Azmi A I & MuhammadN, *Mater Manuf Process,* 31 (2016) 1366.
7 Navarro-MasM D,García-ManriqueJ A, *Materials,*11 (2018) 1418.
8 Patel N, Patel K, Chaudhary V & Gohil V, *AustJMechEng,* 20 (2020)10.
9 Girish D G & DhananjayRM, Parametric *Lasers Manuf Mater,*7 (2020)373.
10 Sathishkumar N, Selvam R, Kumar K M, Abishini A H, Khaleelur Rahman T, & Mohanaranga S, *Mater Today Proc,*62 (2022) 1361.
11 MustafaA& ArmağanAriciA, jet.*Mater Manuf Process,*32 (2017) 1715.
12 RavinderJS, HarpreetS& InderdeepS,*MaterManuf Process,* 29 (2014)370.
13 Navarro M D, Meseguer M D, Sánchez A I& Gutiérrez S C, *Procedia Manuf,*13 259–266.
14 Nima K, KelvinT, WaiN&AmyR*Sustain. Cities and Soc,* 73(2021)e103097.
15 Yuan F, XiaoqingL & Hongyang L, A*J Clean Prod,*328 (2021)e129657.
16 Mohsin A K, ShahMI, Muhammad F J, Ijazm K M, Saim R, El-Shorbagy M A, Essam RE & MalikM Y, *Ain Shams Eng J,* 13 (2022) e101635.
17 Oraléou S D, Akim AS, Zhi-Cong W, JiaD, Lin-Xin Y & Pei-Gao D,. *Energy,* 245 (2022)e123295.
18 Leyre T, Aitor B, Ana B, Jose M L & G, *J Comput Sci,*58 (2022) e101517.
19 Hao P & XiangL, *Int.JHeat Mass Transf,*84 (2015) 203-213.
20 DanielW G, Hitesh B &Sanjoy D, *IntJHeat Mass Transf,*115 (2017) 421.
21 Cai CZ, Pei J F, WenYF, Zhu XJ, Wang GL& Xiao T T, *J. Supercond Nov Magn,*23 (2010) 741
22 ChungaoL, Chongshi G &BoC,*Eng. Comput*.33 (2017) 443-456.

23 ZhouY, LiJ, Sun J & Zhang B, *J Electron,* 29 (2012) 530.
24 Meng W, Xue L,Mei L,Lunbo D &Huicha C, *Ecotoxicol Environ Saf,*233 (2022) e113332.
25 Deva C J, Maheswaran R, AnkitA& Axel B, *J Hydrol,* 613 (2022)e128341.
26 Shouchuan Z, Zheming S, Guangcai W, Rui Y & Zuochen Z, *J Hydrol,*612 (2022) e128249.
27 Chao L,Yankong S,Dazhi Y, Wenting W , Shihuai Z, *Appl Therm Eng,*213 **(**2022) e118675.
28 Tuan N, Jad W, Quy-Dong T, Minh-Ngoc V, *Constr Build Mater*,260 (2020) e119757.
29 AwadM & KhannaR, Support Vector Regression. In: Efficient Learning Machines. *Apress Berkeley CA*, 201567.